Electronic Supplementary Information (ESI) for Chemical Communications

Electronic Supplementary Information

Manipulating AIE ligands into layers of pillar-layered MOFs for enhanced emission

Manman Chang[a], Nan Li[a], Lingxiao Guo[a], Yijia Zhang[a], Xiao-Ting Liu[a]* and Chao Lu[a,b]*

[a] Green Catalysis Center, and College of Chemistry, Zhengzhou University, Zhengzhou, 450001, China.

[b] State Key Laboratory of Chemical Resource Engineering, Beijing University of Chemical Technology, Beijing, 100029, China

*Corresponding author:

liuxiaoting@zzu.edu.cn (X.-T. Liu), luchao@mail.buct.edu.cn (C. Lu).

Postal address: Green Catalysis Center, and College of Chemistry, Zhengzhou University, Zhengzhou, 450001, China.

Materials and Instrumentation

All chemical reagents and solvents were purchased from commercial sources and used as received without further purification.

Single crystal X-ray analysis of compounds **1**-**5** were performed on a Bruker D8 Venture diffractometer Cu-Ka radiation (λ = 1.54178 Å) at 173 K. The structures were solved by intrinsic phasing methods using SHELXT program. Refining programs were performed using SHELXL-2018/3, and final full-matrix refinements were against F^2.[1] The crystallographic data are listed in Table S1-S2. The CCDC numbers are 2344301, 2344303, 2344304, 2344305 and 2344306, respectively. The selected bond lengths and bond angles are listed in Table S3-S7.

Powder X-ray diffraction (PXRD) patterns were acquired on a Rigaku MiniFlex 600 diffractometer with Cu Kαradiation over the range from 3 to 50^o at the air atmosphere. Variable-temperature PXRD were performed on a Bruker D8 Advance diffractometer from 30 to 400 ^{o}C over the range from 3 to 50^o at the air atmosphere. Thermogravimetric analysis (TGA) was performed on a Setline STA thermal analyzer at a heating speed of 10 °C/min from room temperature to 800 °C at air atmosphere. The ^{1}H NMR spectra were measured on a Bruker AVANCE III HD 400 M spectrometer. The UV-Vis spectra were collected at a UV-2700i spectrophotometer. The luminescent spectra were performed on an Edinburgh instrument FLS1000 fluorescence spectrometer. The PL decay curves were measured with the FLS1000 fluorescence spectrometer and a 365 nm laser as excitation source. The absolute quantum yield (QY) values were measured with the FLS1000 fluorescence spectrometer by using an integrating sphere.

Experimental procedure

Synthesis of compound **1**. A mixture of $Cd(NO_3)_2{\cdot}4H_2O$ (12.34 mg, 0.04 mmol), H_4TCPP (11.68 mg, 0.02 mmol), 4 mL of DMF, 2 mL of H_2O and five drops of HBF_4 were added in a 10 mL vital. The vital was capped and heated at 95 ℃ for 72 h and colorless transparent biconical crystals can be obtained.

Synthesis of compounds **2**-**5.** Compounds **2**-**5** were obtained by the similar method as compound **1**, except for additional adding L_1 (3.12 mg, 0.02 mmol), L_2 (3.64 mg, 0.02 mmol), L_3 (3.68 mg, 0.02 mmol) and L_4 (4.65 mg, 0.02 mmol) in the corresponding mixed solutions.

The digest ^{1}H NMR experiments were performed by dissolving 5 mg of these five samples in 400 μL of DMSO-*d6* with 20 μL trifluoroacetic acid-*d* mixed solution.

Thermal stability analysis

The TGA curve of compound **1** shows a continuous weight loss from the room temperature to 320 ^{o}C caused by the free solvent molecules' loss and a sharp decrease of weight loss occurs after 320 ^{o}C, responding to the collapse of the framework. Variable-temperature PXRD patterns indicate the crystallinity can be maintained to 180 ^{o}C. Compound **2** exhibits a slow weight loss from room temperature to 350 ^{o}C and a sharp weight loss after 350 ^{o}C obtained from TGA curve. Variable-temperature PXRD result indicates compound **2** can maintain its crystallinity to 350 ^{o}C. Compared with compound **1**, the higher thermal stability of **2** may be caused by the L_1-induced formation of interpenetration network. The TGA curve of compound **3** exhibits a slow weight loss before 275 ^{o}C and a sharp weight loss after 400 ^{o}C, and variable-temperature PXRD patterns indicates the crystallinity can maintain to 400 ^{o}C. The enhanced stability can be attributed to the relatively rigid framework nature originating from the rigid L_2 pillaring ligands. Compounds **4** and **5** also exhibit improved thermal stability compared with compound **1**. The TGA curve of compound **4** reveals a continuous loss of weight before 290 ^{o}C and a sharp weight loss after 350 ^{o}C. Variable-temperature PXRD data exhibits compound **4** can maintain its crystallinity to 210 ^{o}C. The TGA curve of compound **5** reveals a continuous loss of weight before 295 ^{o}C and a sharp weight loss after 375 ^{o}C. Variable-temperature PXRD data exhibits compound **5** can maintain its crystallinity to 240 ^{o}C. Considering the similar structure character of compounds **4** and **5**, the slightly thermal stability increases of compound **5** can be attributed to the relatively rigid framework induced by L_4 relative to L_3 pillaring ligand.

Verification of the existence of $[(CH_3)_2NH_2]^+$ cation in compound 1

To verify the presence or absence of $[(CH_3)_2NH_2]^+$ cation in compounds **1**-**5**, the digest ^{1}H NMR of these five samples were performed. Results reveal there exists $[(CH_3)_2NH_2]^+$ cation in compound **1** while there is no $[(CH_3)_2NH_2]^+$ cation in compounds **2**-**5**, which may be originating from the existence of pillar ligands L_1-L_4 that influence the reaction microenvironment (Fig. S11-S15).

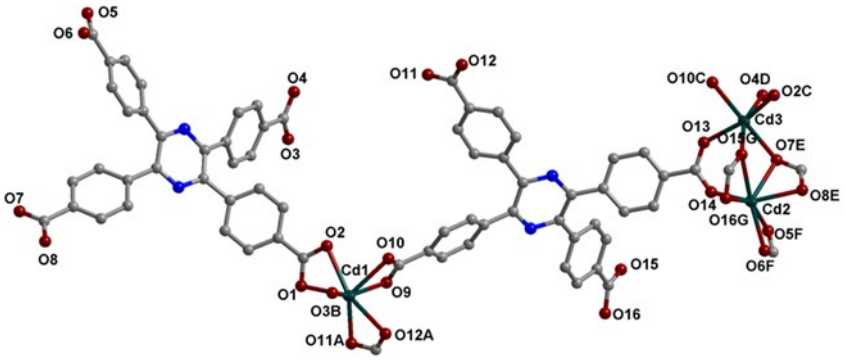

Figure S1. Coordination environment of Cd(II) and $TCPP^{4-}$ ligands in compound **1** ($\{[(CH_3)_2NH_2]_4[Cd_6(TCPP)_4]\}_n \cdot nDMF$). (symmetric codes: A (x, -1+y, z), B (-1+x, y, z), C (-x, 2-y, 1-z), D (1-x, 2-y, 1-z), E (-1+x, 1+y, 1+z), F (-1+x, y, 1+z), G (-1+x, 1+y, z)).

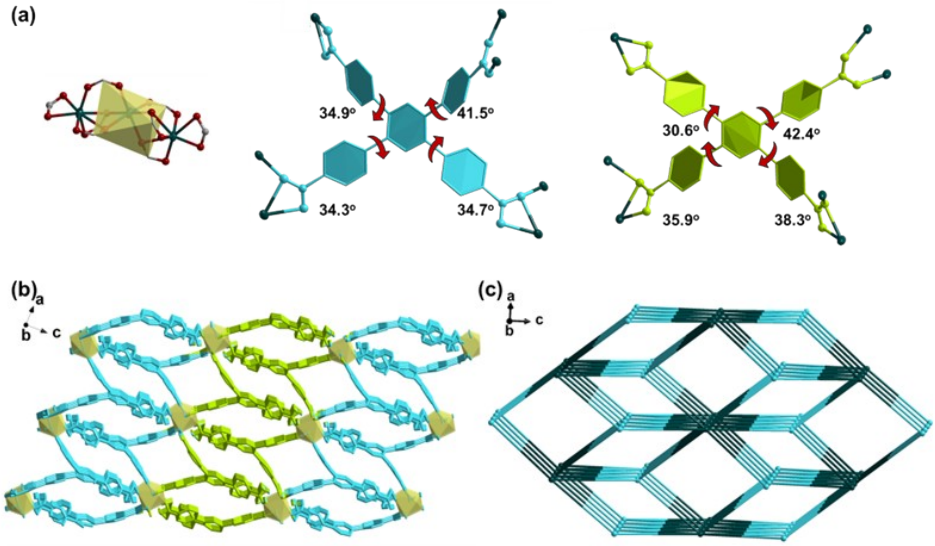

Figure S2. The crystal structure of compound **1**. (a) The trinuclear SBU and coordination modes of the two $TCPP^{4-}$ ligands with different conformations; (b) The 3D framework structure; (c) Topological network. (All hydrogen atoms, free DMF molecules and $[(CH_3)_2NH_2]^+$ ions are omitted for clarity.)

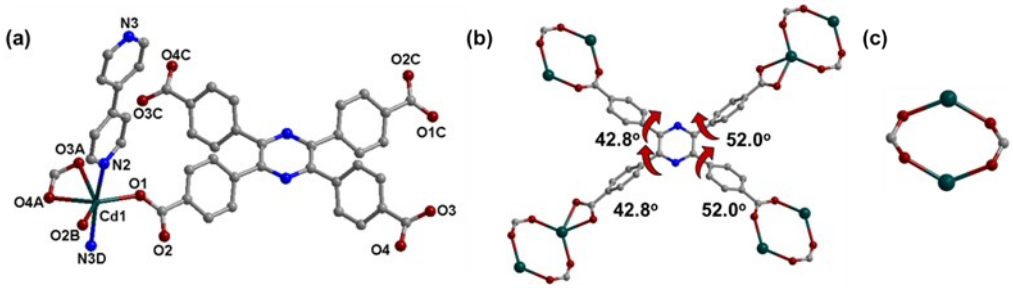

Figure. S3. The crystal structure of compound **2** ($[Cd(TCPP)_{0.5}(L_1)]_n \cdot nDMF$). (a) Coordination environment of Cd(II), $TCPP^{4-}$ and L_1 ligands (symmetric codes: A (-1+x, -1+y, z), B (1-x, -y, 2-z), C (2-x, 1-y, 1-z), D (1+x, -1+y, z); (b) Coordination mode of the $TCPP^{4-}$ ligands with the dihedral angles of the four phenyl rings and the pyrazine ring; (c) The binuclear SBU.

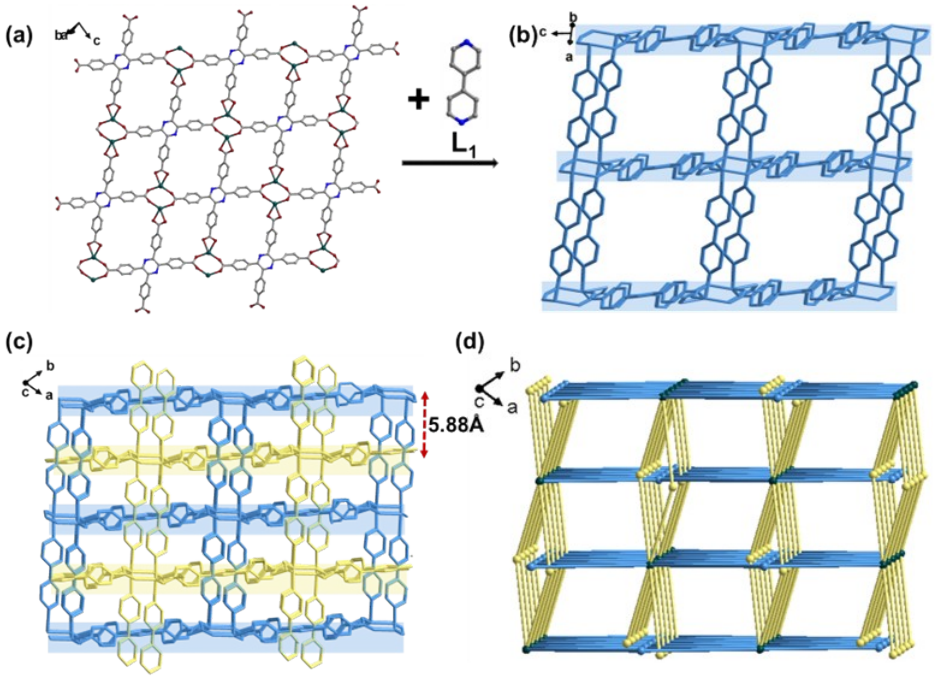

Figure S4. The crystal structure of compound **2**. (a) The 2D coordination sheet; (b) The 3D pillar-layered network; (c) The 2-fold interpenetrated 3D pillar-layered structure; (d) Topological network. (All hydrogen atoms and free DMF molecules are omitted for clarity.)

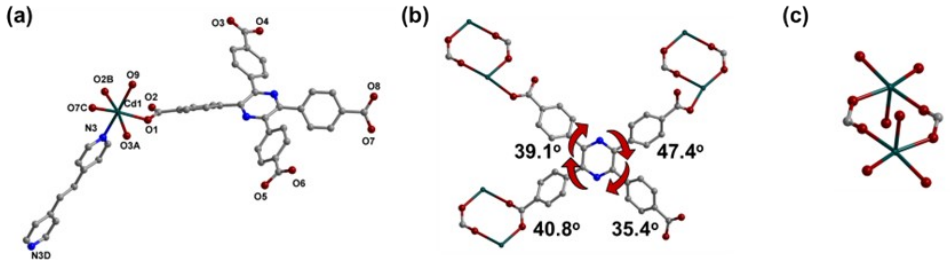

Figure. S5. The crystal structure of compound **3** ($[Cd(H_2TCPP)(L_2)_{0.5}(H_2O)]_n \cdot nDMF$). (a) Coordination environment of Cd(II), H_2TCPP^{2-} and L_2 ligands (symmetric codes: A (x, 1+y, z), B (1-x, 1-y, -z), C (x, 1+y, -1+z), D (-x, 2-y, -z); (b) Coordination mode of the H_2TCPP^{2-} ligands with the dihedral angles of the four phenyl rings and the pyrazine ring; (c) The binuclear SBU.

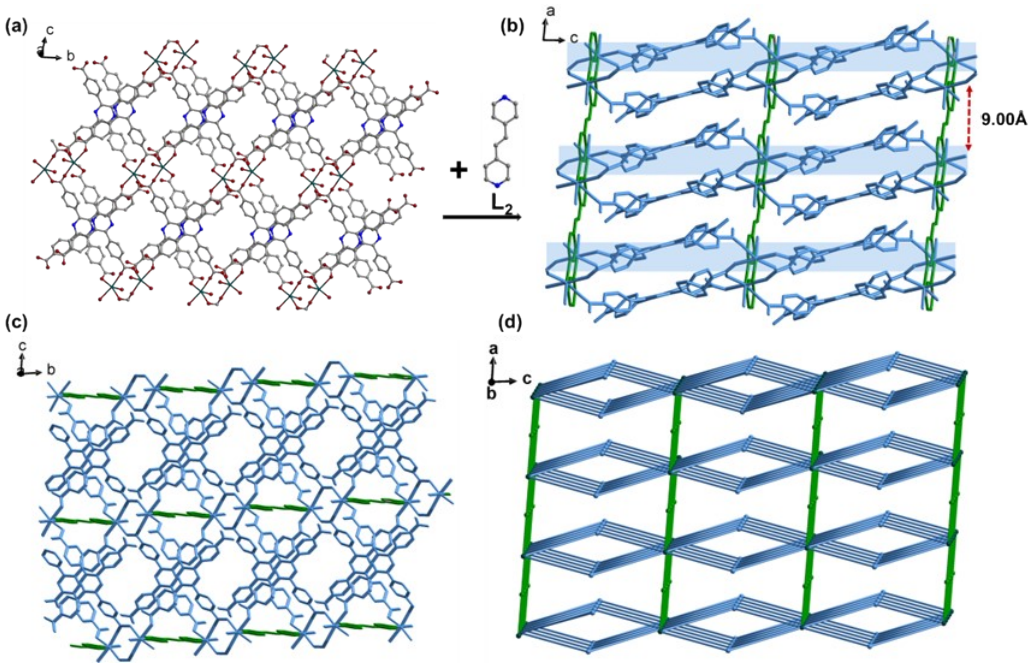

Figure S6. The crystal structure of compound **3**. (a) The 2D bilayer network; (b) The 3D pillar-layered structure viewing along b axis; (c) The 3D pillar-layered structure viewing along a axis; (d) Topological network. (All hydrogen atoms and free DMF molecules are omitted for clarity.)

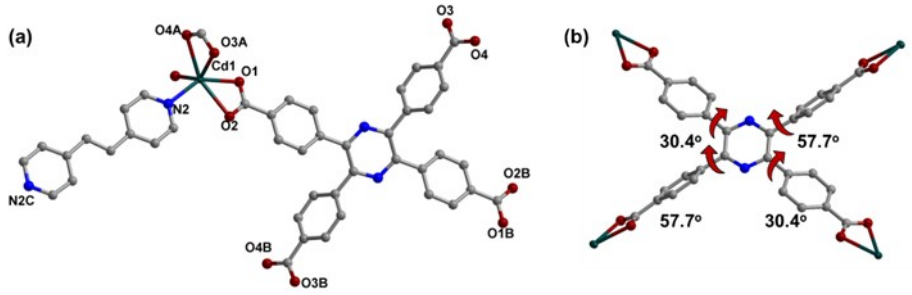

Figure. S7. The crystal structure of compound **4** ($[Cd_4(TCPP)_2(L_3)_2(H_2O)_4]_n \cdot 4nDMF$). (a) Coordination environment of Cd(II), $TCPP^{4-}$ and L_3 ligands (symmetric codes: A (0.5-x, -1.5+y, 0.5-z), B (0.5-x, 2.5-y, 1-z), C (1-x, -1-y, 1-z); (b) Coordination mode of the $TCPP^{4-}$ ligands with the dihedral angles of the four phenyl rings and the pyrazine ring.

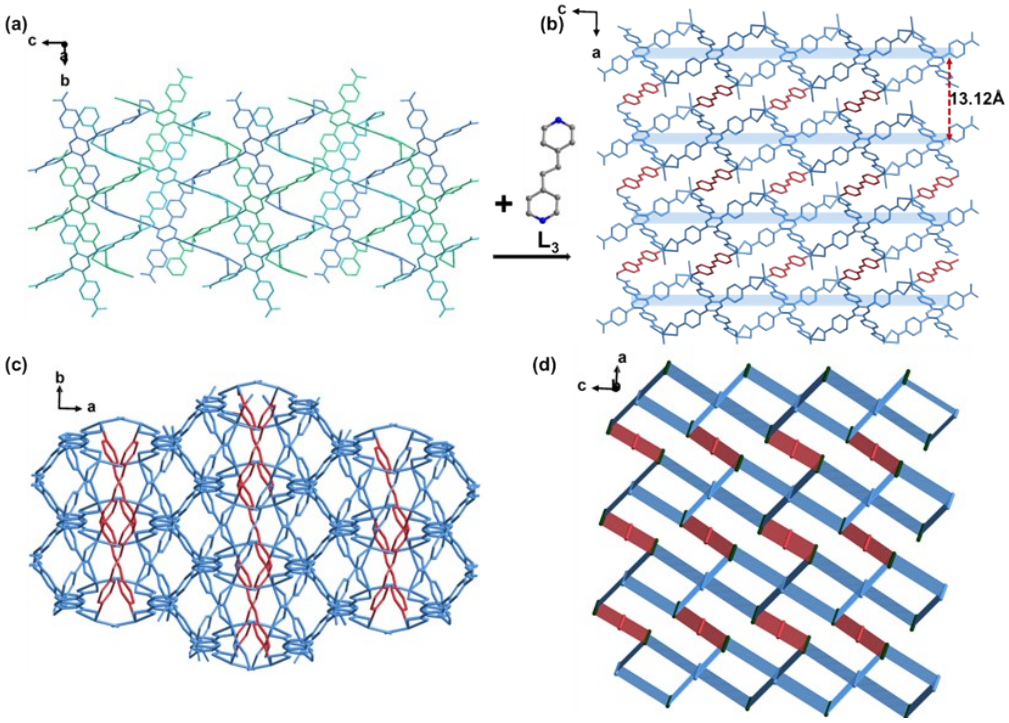

Figure S8. The crystal structure of compound **4**. (a) The 2D trilayer woven structures; (b) The 3D pillar-layered structure viewing along b axis; (c) The 3D pillar-layered structure viewing along c axis; (d) Topological network. (All hydrogen atoms and free DMF molecules are omitted for clarity.)

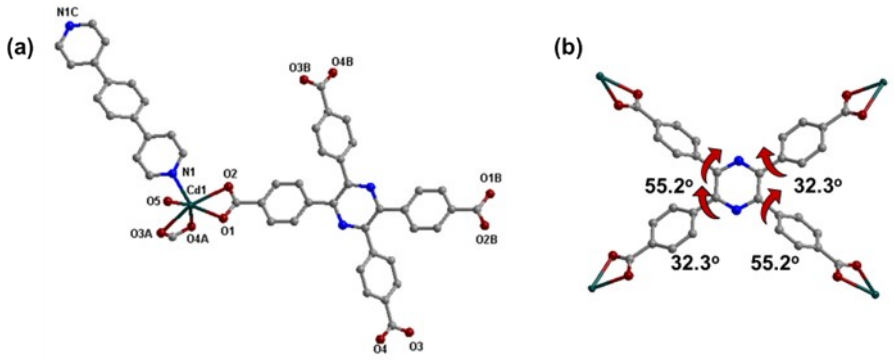

Figure. S9. The crystal structure of compound **5** ($[Cd_4(TCPP)_2(L_4)_2(H_2O)_4]_n \cdot 4nDMF$). (a) Coordination environment of Cd(II), $TCPP^{4-}$ and L_4 ligands (symmetric codes: A (0.5-x, -1.5+y, 0.5-z), B (0.5-x, 2.5-y, 1-z), C (1-x, -1-y, 1-z); (b) Coordination mode of the $TCPP^{4-}$ ligands with the dihedral angles of the four phenyl rings and the pyrazine ring.

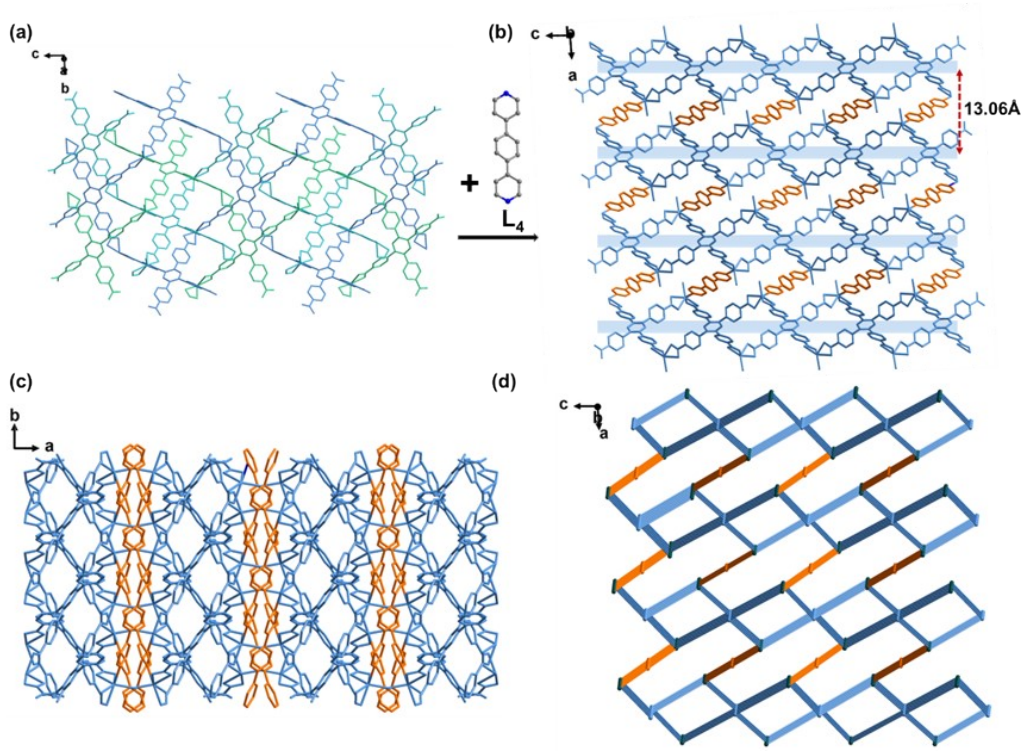

Figure S10. The crystal structure of compound **5**. (a) The 2D trilayer woven structures; (b) The 3D pillar-layered structure viewing along b axis; (c) The 3D pillar-layered structure viewing along c axis; (d) Topological network. (All hydrogen atoms and free DMF molecules are omitted for clarity.)

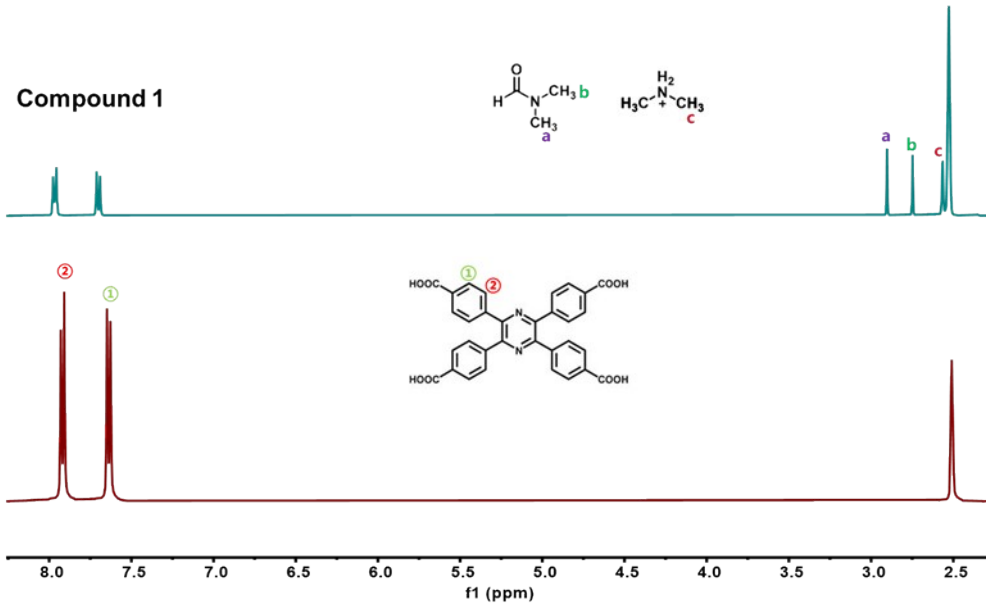

Figure S11. The ^{1}H NMR spectra of digested compound **1** samples and H_4TCPP ligand.

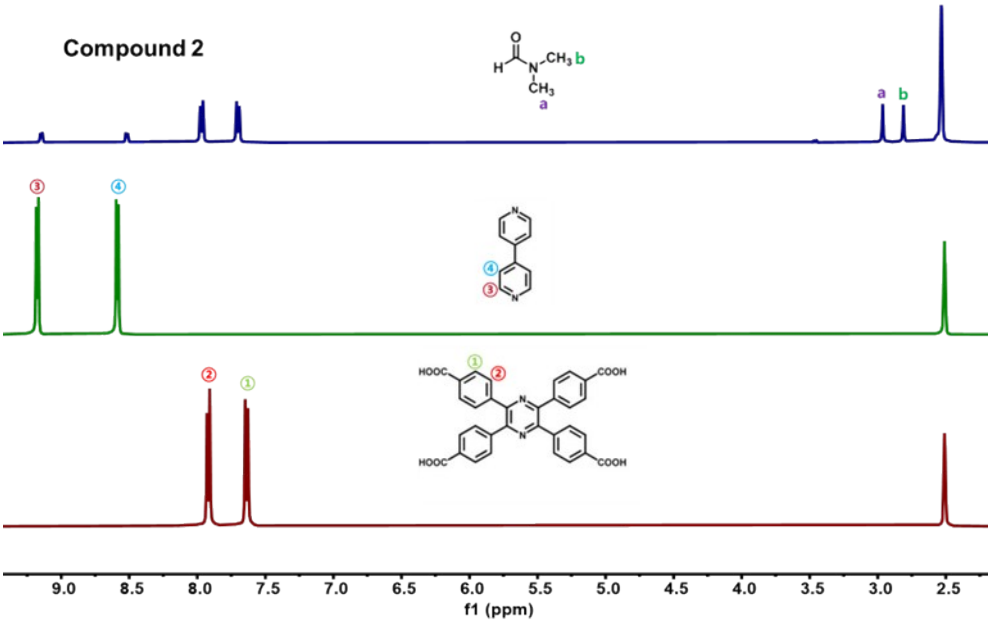

Figure S12. The ^{1}H NMR spectra of digested compound **2** samples, H_4TCPP and L_1 ligands.

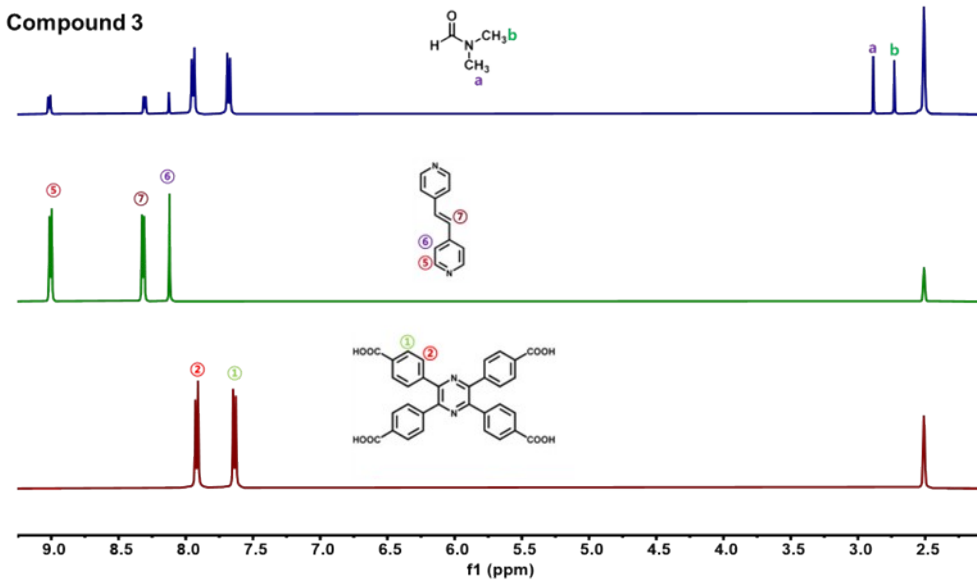

Figure S13. The ^{1}H NMR spectra of digested compound **3** samples, H_4TCPP and L_2 ligands.

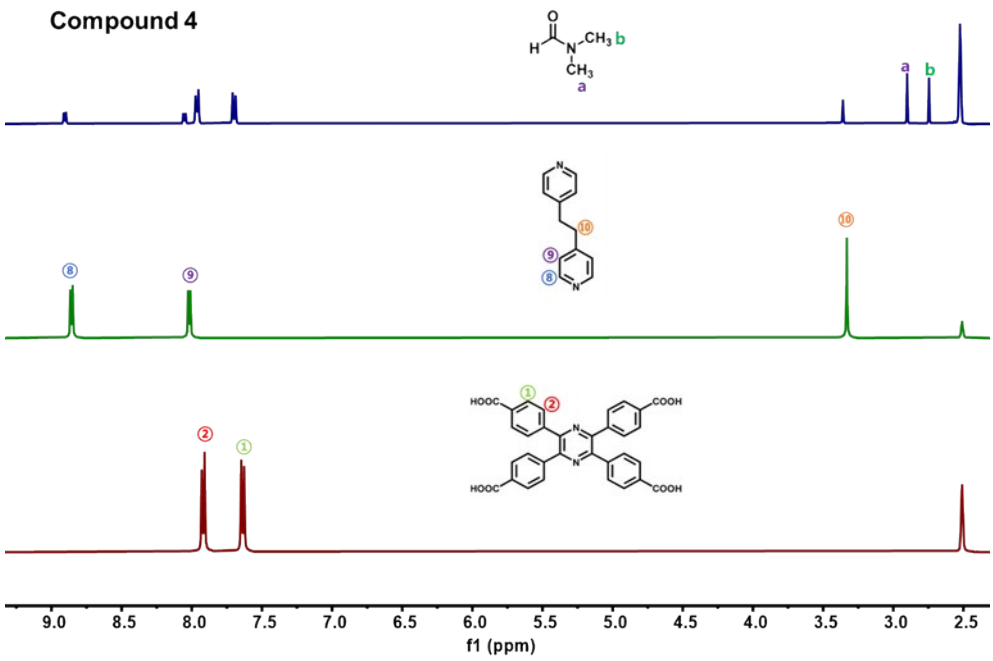

Figure S14. The ^{1}H NMR spectra of digested compound **4** samples, H_4TCPP and L_3 ligands.

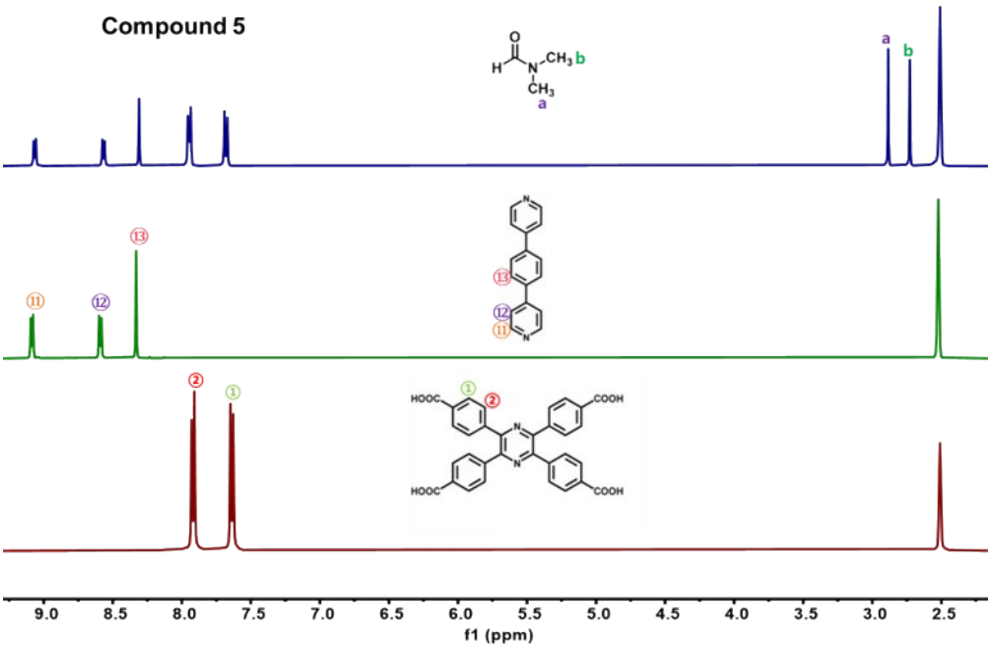

Figure S15. The ^{1}H NMR spectra of digested compound **5** samples, H_4TCPP and L_4 ligands.

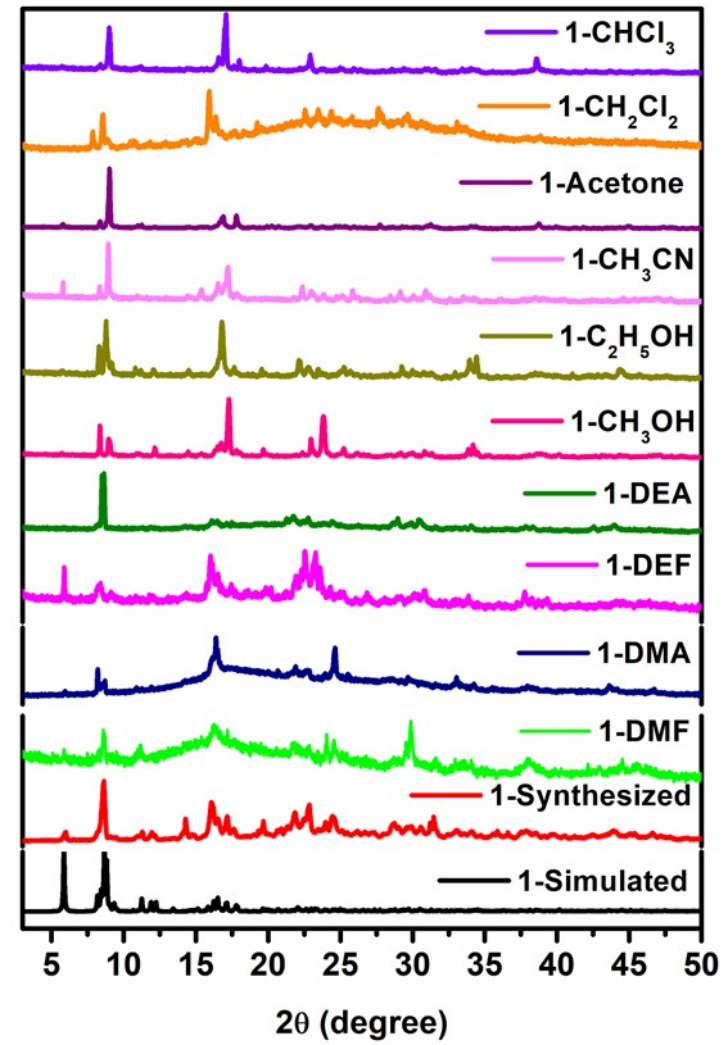

Figure. S16. The PXRD patterns of the synthesized powder sample of **1** immersed in different solvents for 24 h, with the simulation as reference.

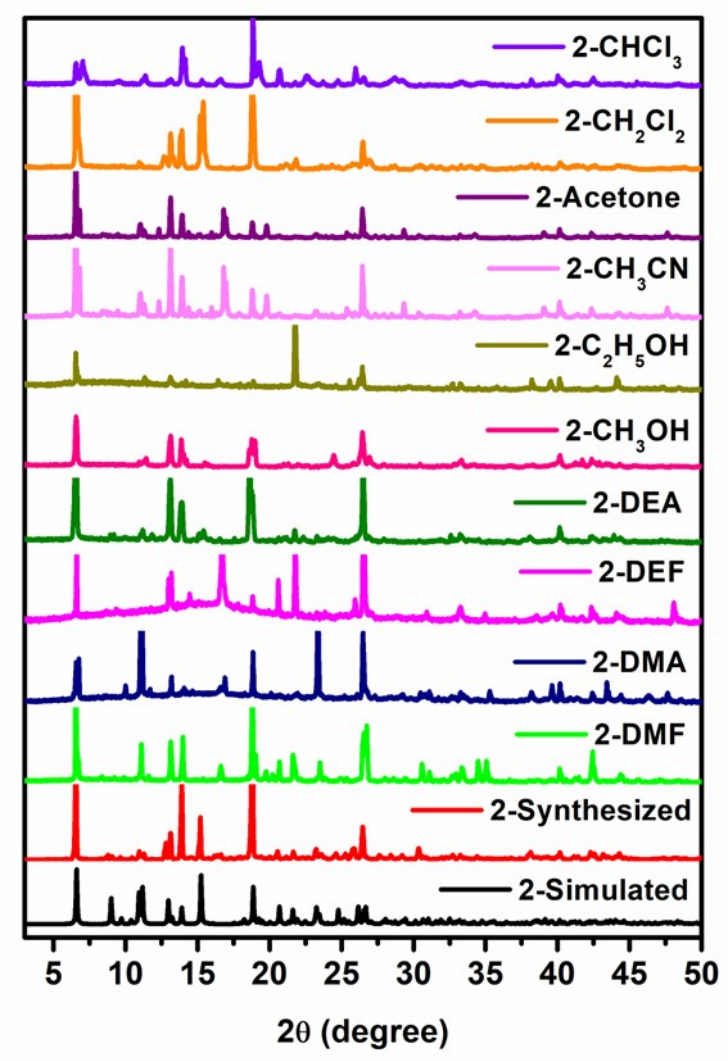

Figure. S17. The PXRD patterns of the synthesized powder sample of **2** immersed in different solvents for 24 h, with the simulation as reference.

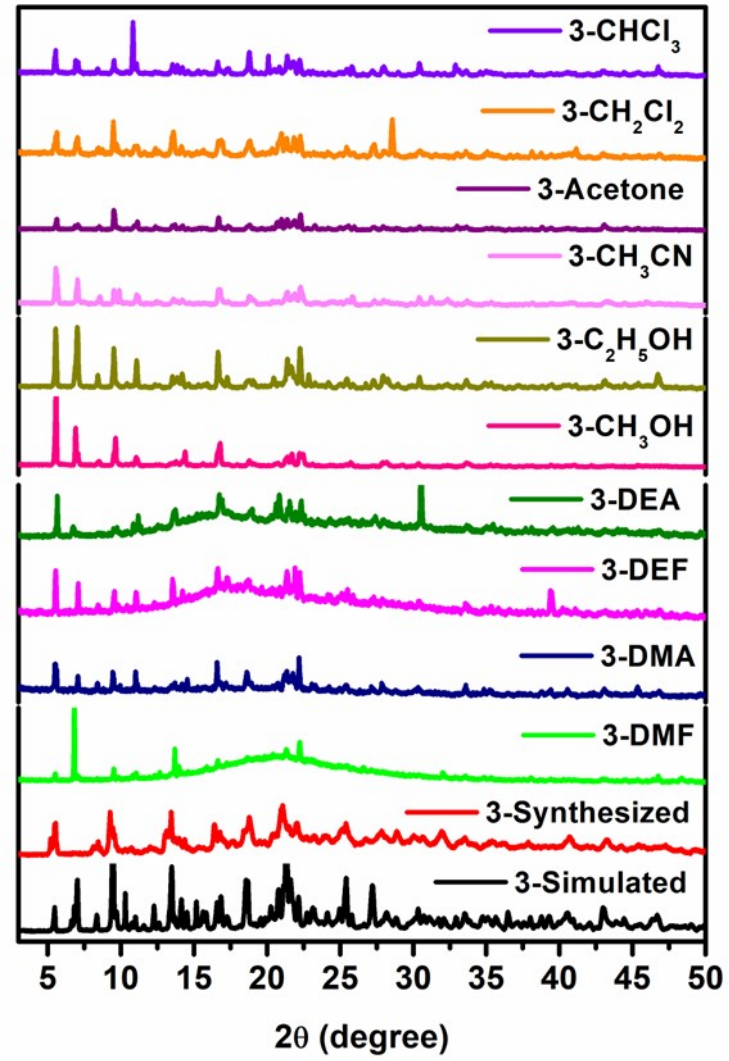

Figure. S18. The PXRD patterns of the synthesized powder sample of **3** immersed in different solvents for 24 h, with the simulation as reference.

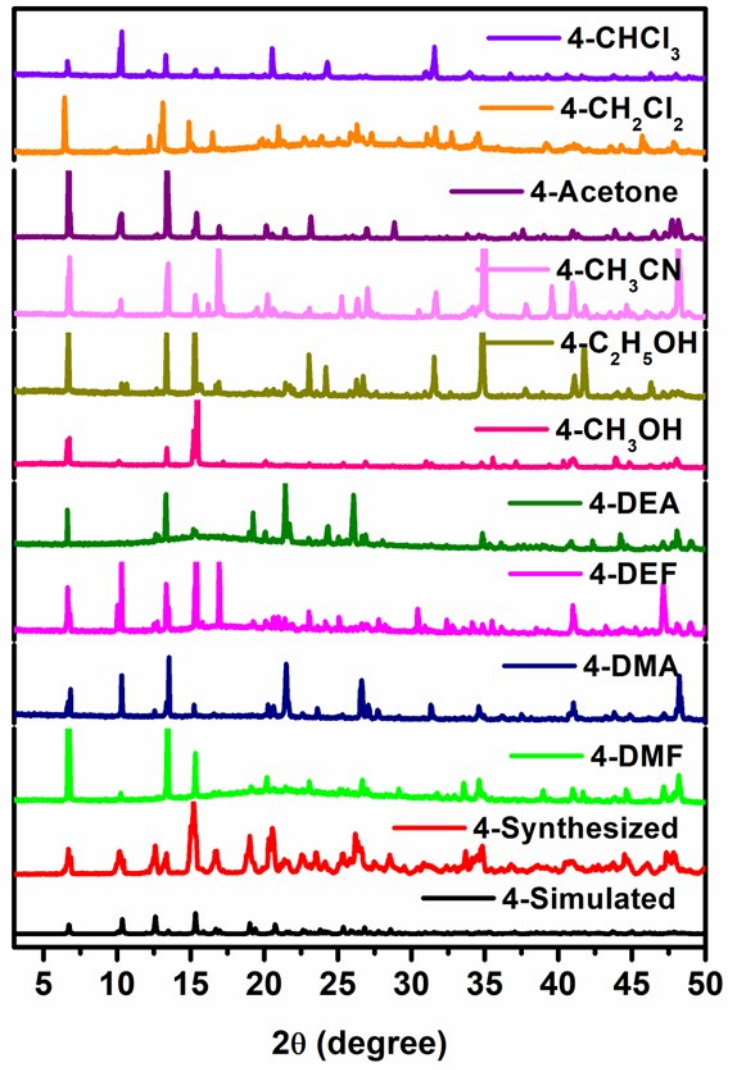

Figure. S19. The PXRD patterns of the synthesized powder sample of **4** immersed in different solvents for 24 h, with the simulation as reference.

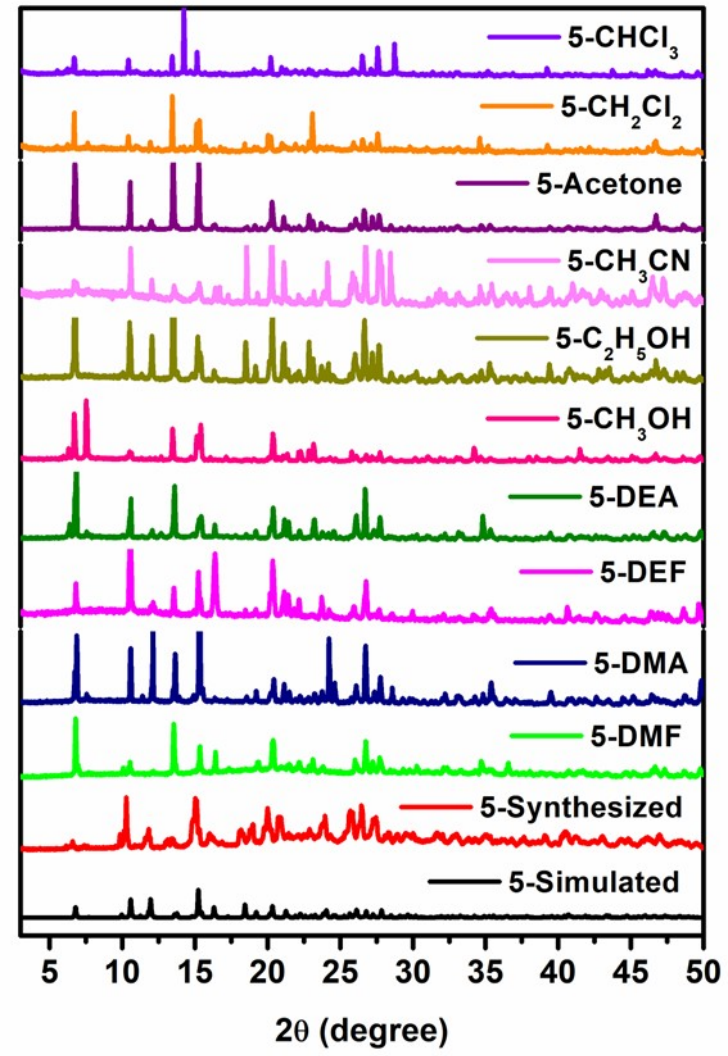

Figure. S20. The PXRD patterns of the synthesized powder sample of **5** immersed in different solvents for 24 h, with the simulation as reference.

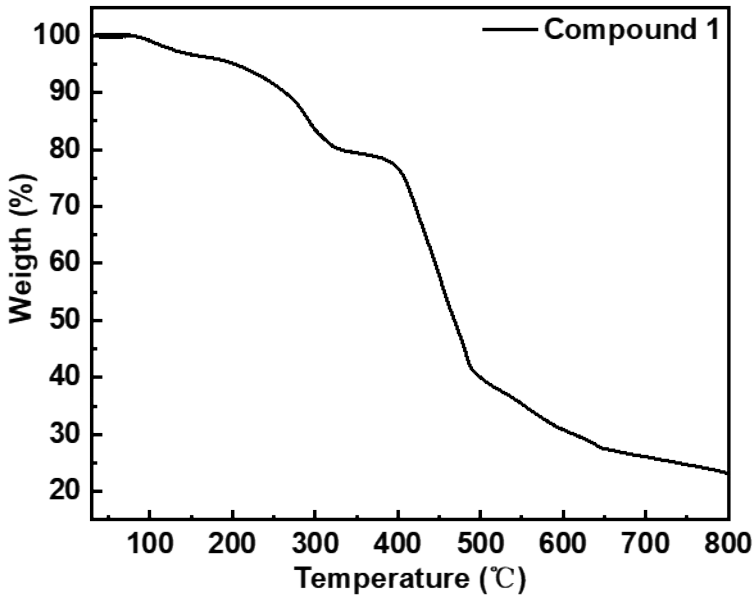

Figure. S21. The TGA curve of compound **1**.

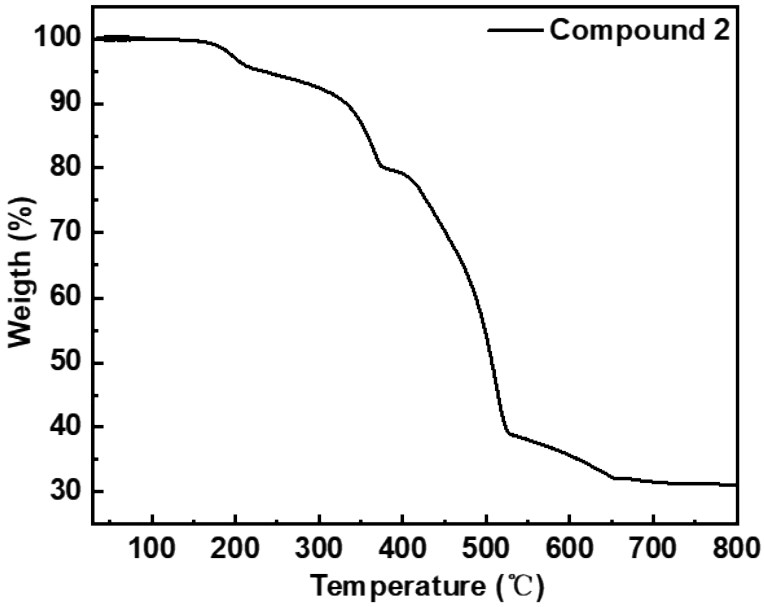

Figure. S22. The TGA curve of compound **2**.

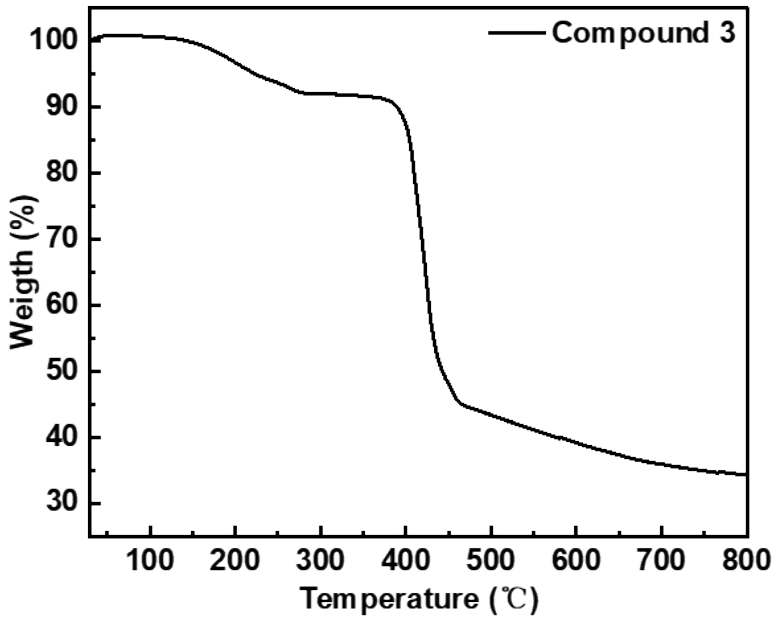

Figure. S23. The TGA curve of compound **3**.

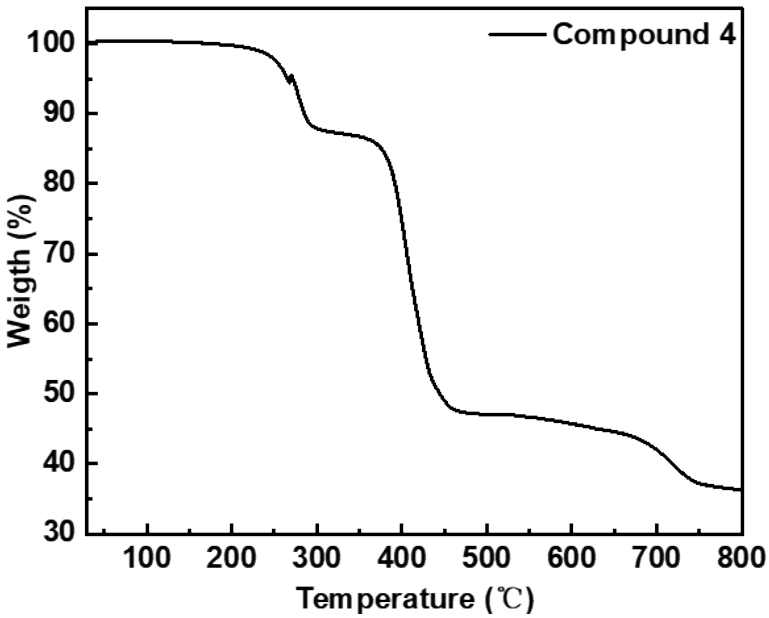

Figure. S24. The TGA curve of compound **4**.

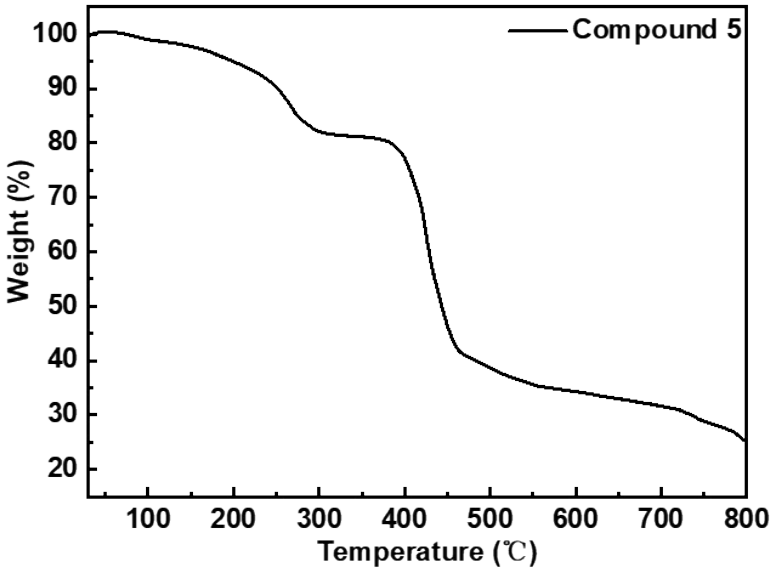

Figure. S25. The TGA curve of compound **5**.

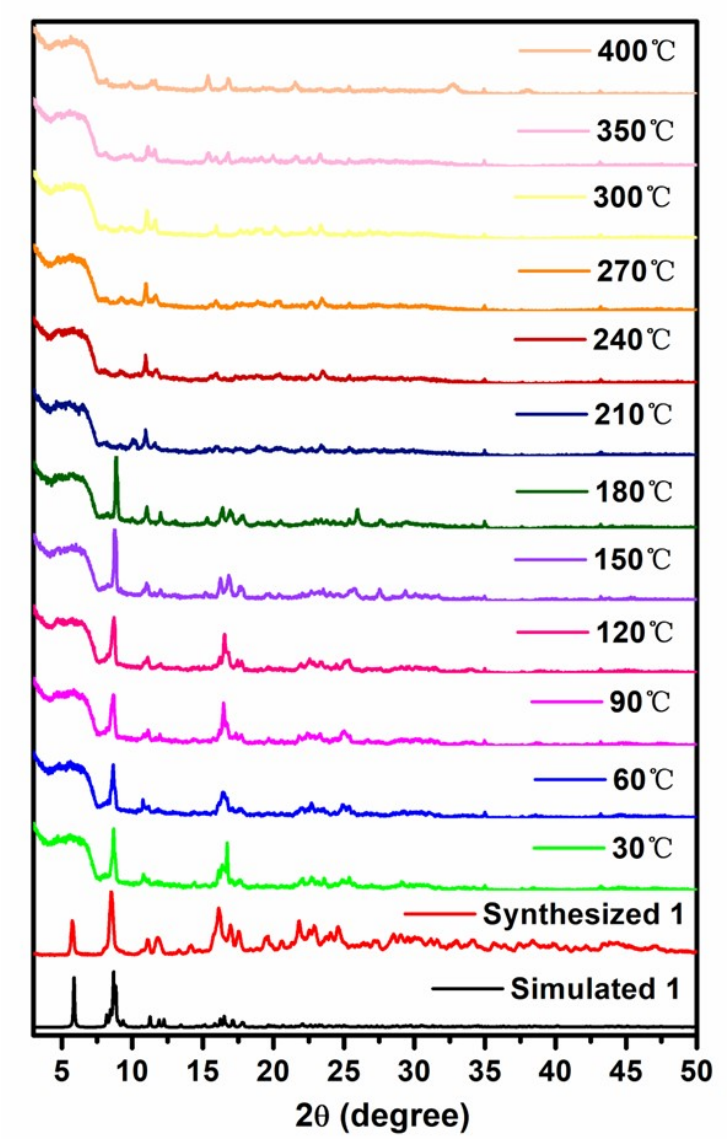

Figure. S26. The variable-temperature PXRD patterns of the powder sample of compound **1**.

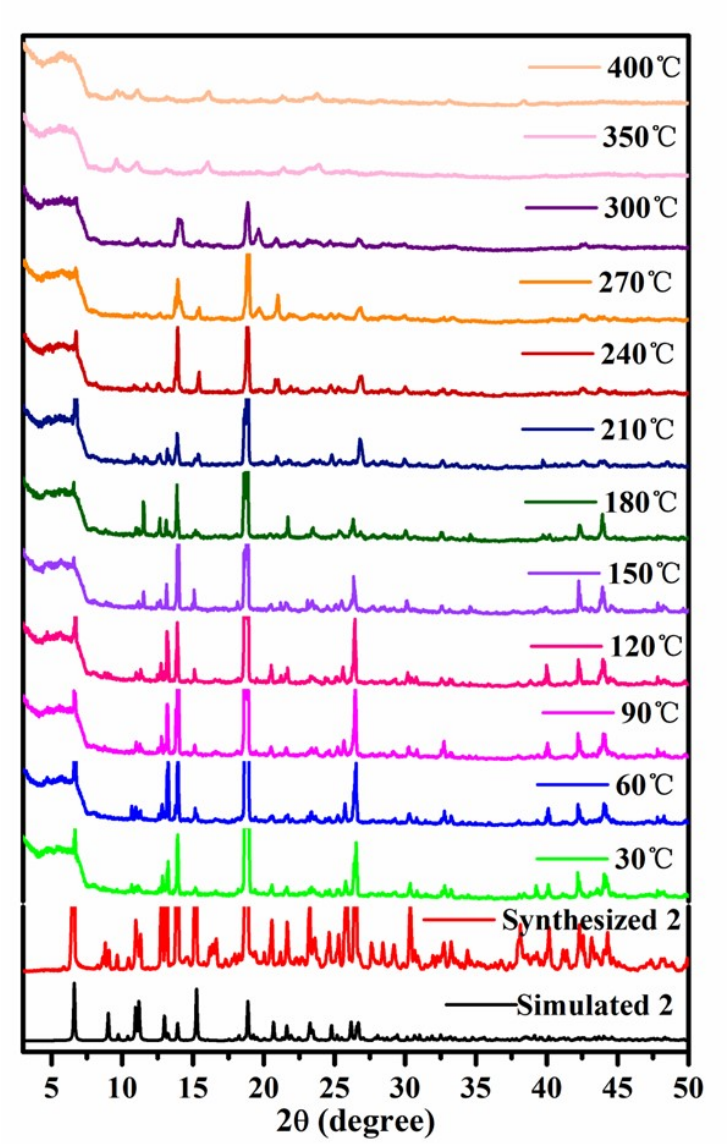

Figure. S27. The variable-temperature PXRD patterns of the powder sample of compound **2**.

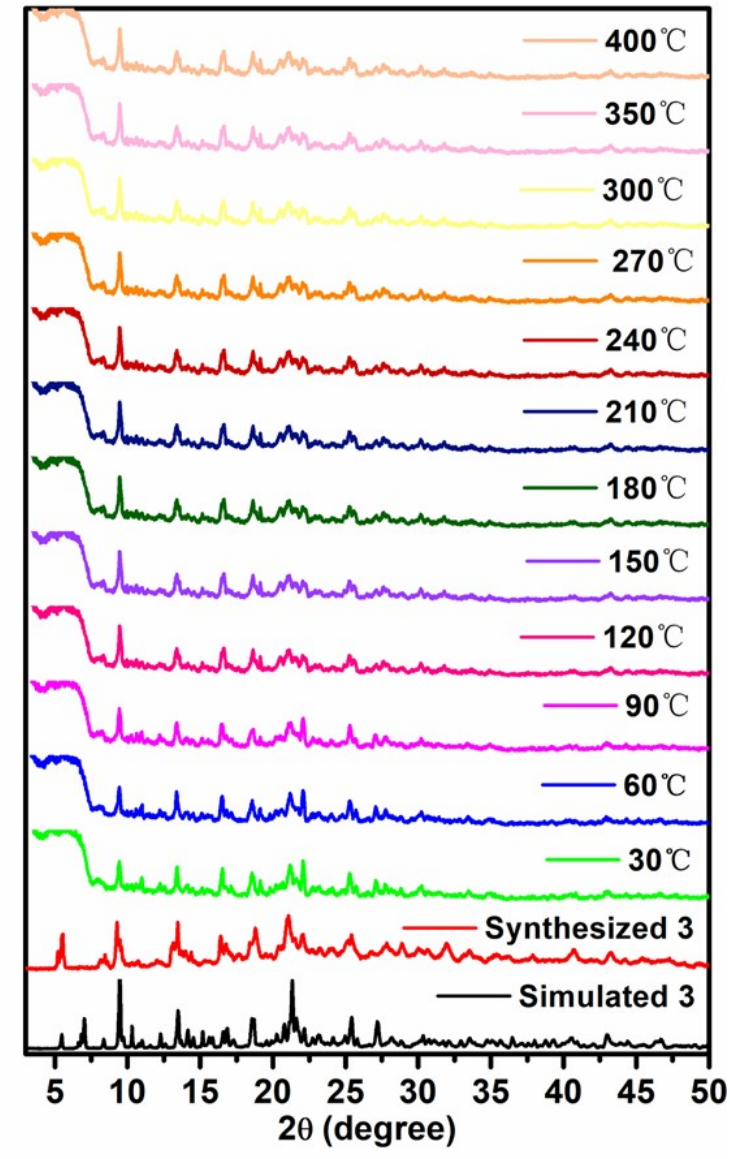

Figure. S28. The variable-temperature PXRD patterns of the powder sample of compound **3**.

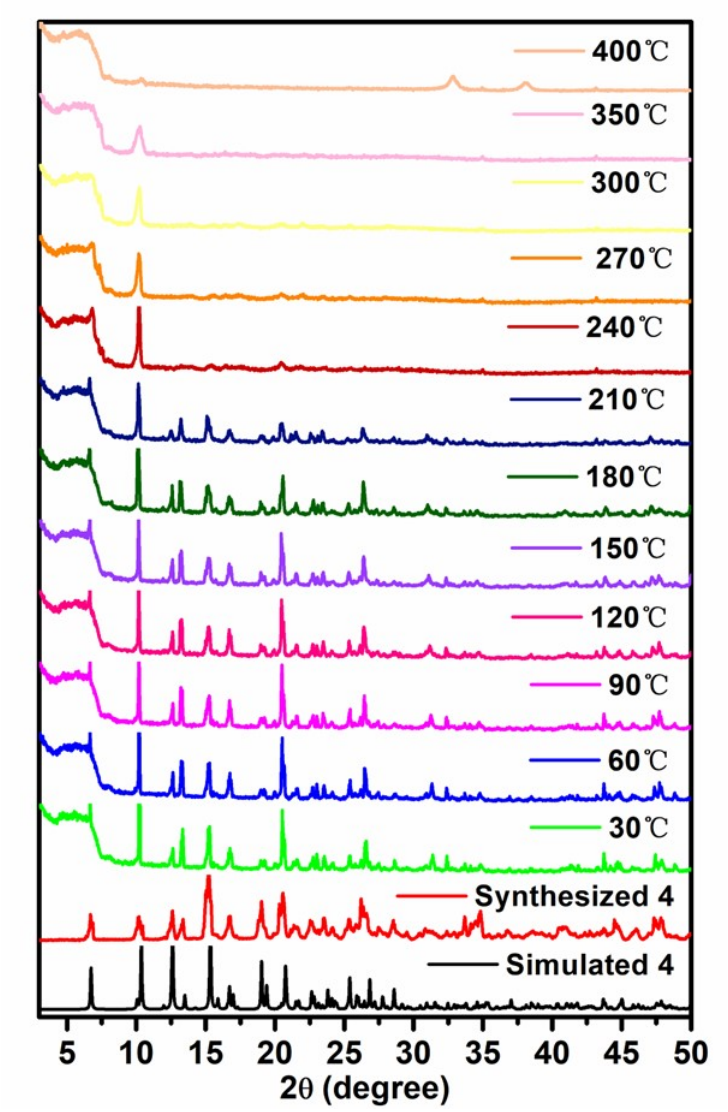

Figure. S29. The variable-temperature PXRD patterns of the powder sample of compound **4**.

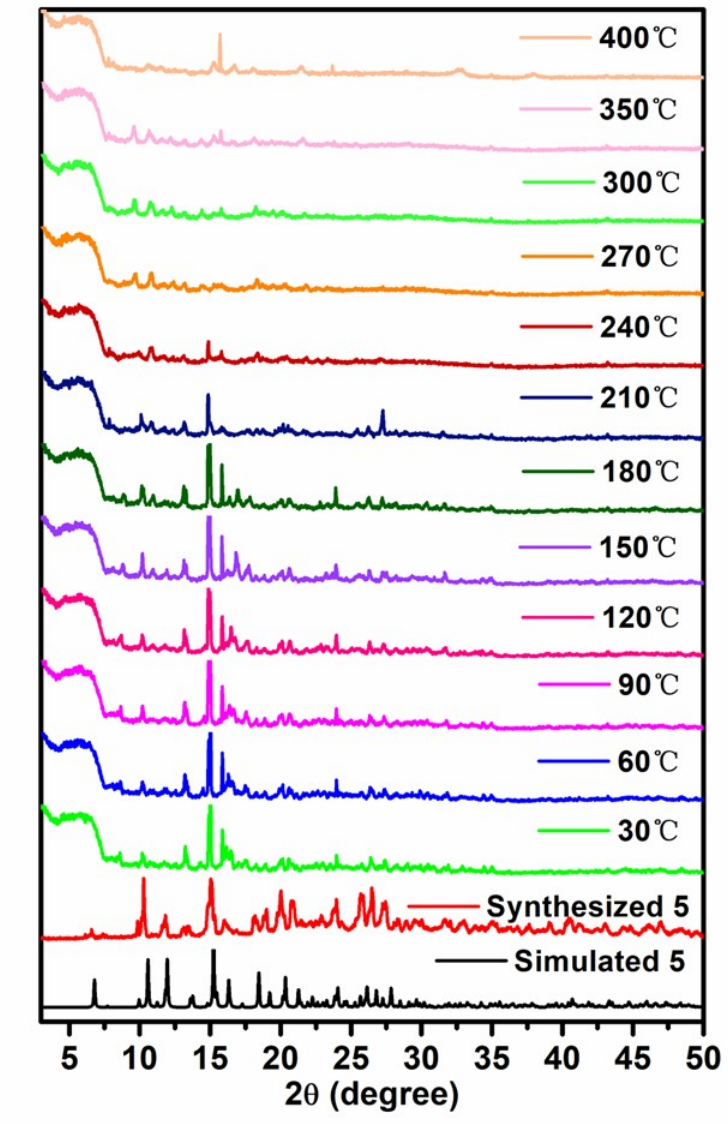

Figure. S30. The variable-temperature PXRD patterns of the powder sample of compound **5**.

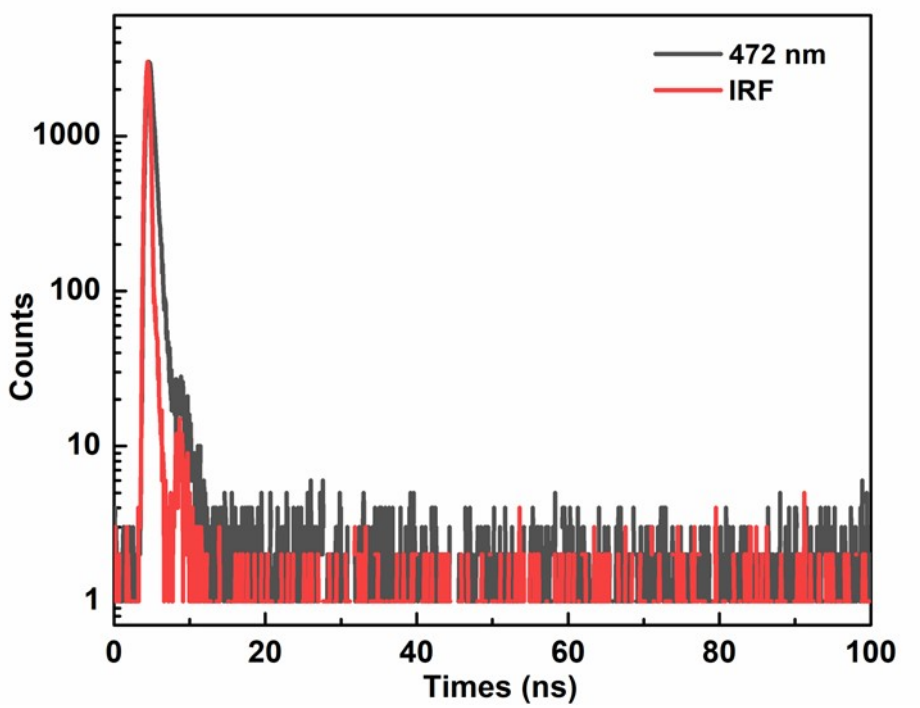

Figure. S31. The luminescent decay curve of H_4TCPP solid sample at 472 nm.

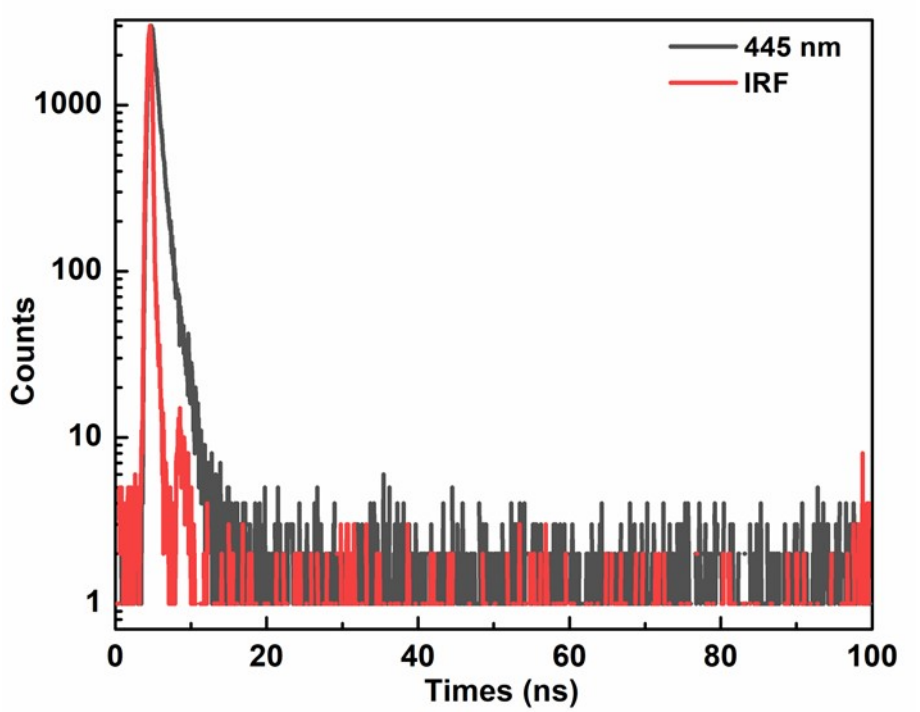

Figure. S32. The luminescent decay curve of compound **1** at 445 nm.

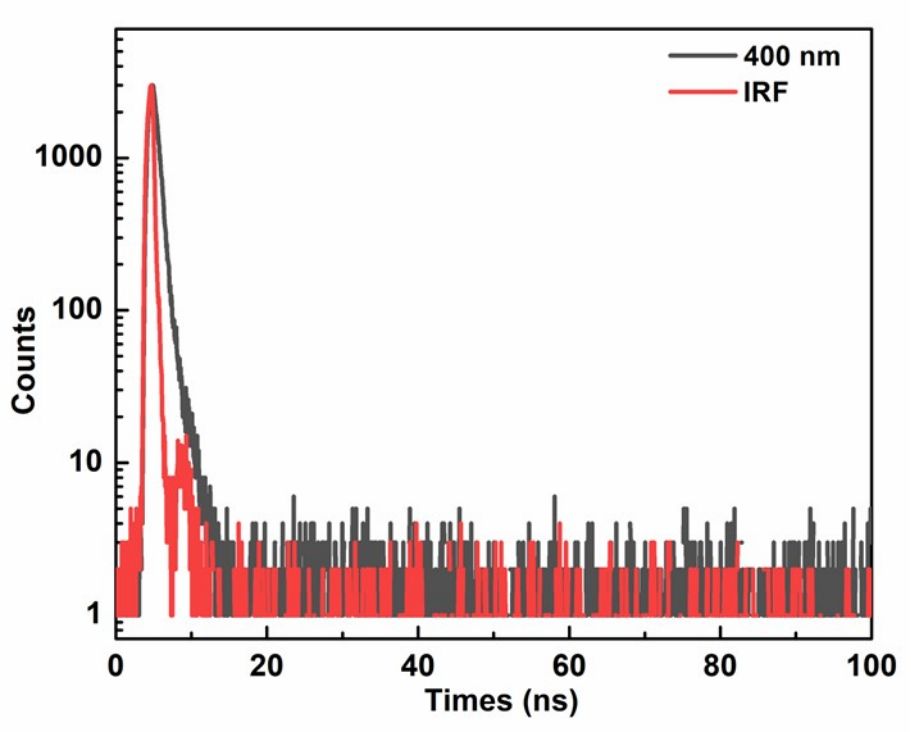

Figure. S33. The luminescent decay curve of compound **2** at 400 nm.

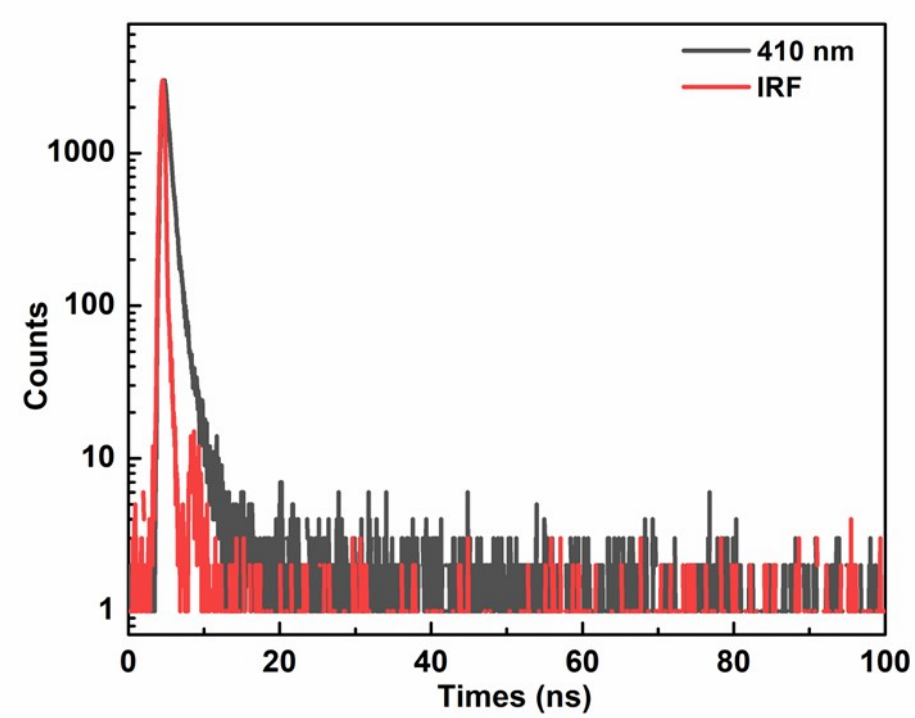

Figure. S34. The luminescent decay curve of compound **3** at 410 nm.

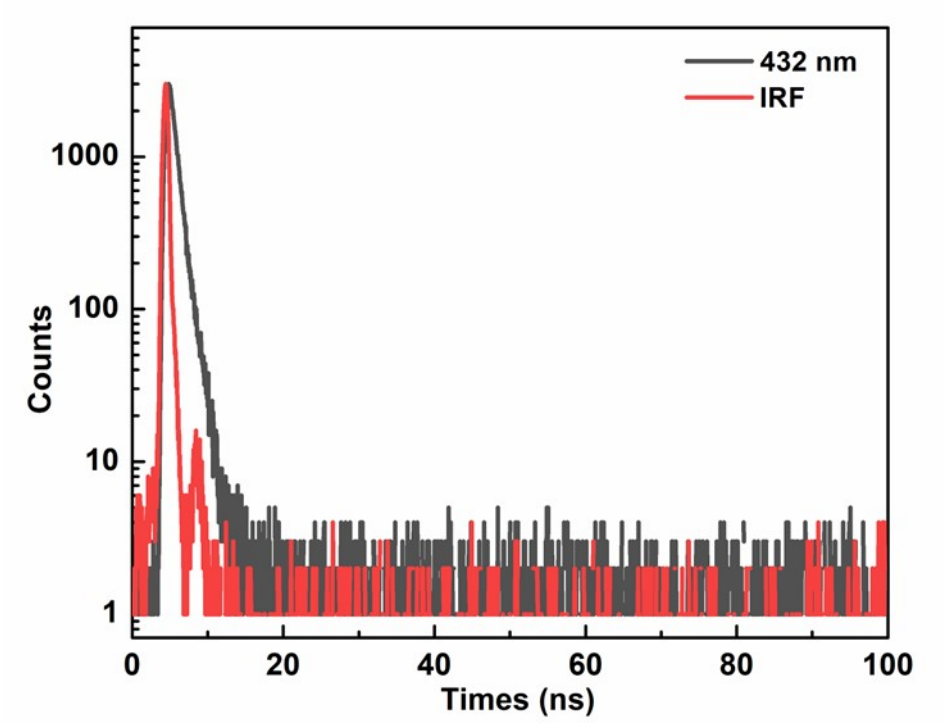

Figure. S35. The luminescent decay curve of compound **4** at 432 nm.

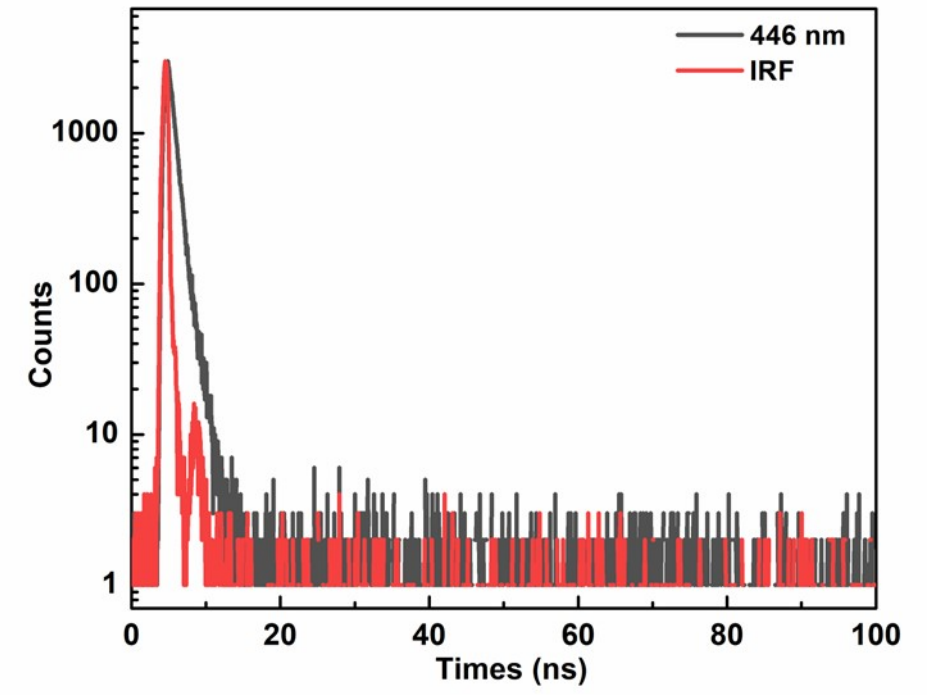

Figure. S36. The luminescent decay curve of compound **5** at 446 nm.

Table S1. Crystal data and structure refinement for compounds **1**-**3**.

	Compound **1**	Compound **2**	Compound **3**
Empirical Formula	$C_{139}H_{103}Cd_6N_{13}O_{33}$	$C_{29}H_{23}CdN_4O_5$	$C_{41}H_{32}CdN_4O_{10}$
Formula weight	3157.74	619.91	853.10
Temperature/K	173.0	173.0	173.0
Wavelength/Å	1.54178	1.54178	1.54178
Crystal system	Triclinic	Triclinic	Triclinic
Space group	$P\bar{1}$	$P\bar{1}$	$P\bar{1}$
θ/º	4.098 to 73.685	3.307 to 74.623	2.771 to 72.200
a/Å	12.2239(8)	9.8998(5)	9.0027(2)
b/Å	12.3893(7)	10.3818(5)	12.5556(2)
c/Å	30.5039(16)	13.7847(7)	16.1594(3)
α/°	80.911(3)	85.545(2)	82.3970(10)
β/°	84.233(3)	75.783(2)	84.3170(10)
γ/°	61.359(3)	70.838(2)	87.2620(10)
V/Å^3	4001.9 (4)	1297.27(11)	1800.50(6)
Z	1	2	2
D_c/g·cm^{-3}	1.310	1.587	1.574
μ/mm^{-1}	6.843	7.143	5.436
F (000)	1580	626	868
R_1 (I >2σ(I))	0.1316	0.0398	0.0413
wR_2 (all data)	0.3808	0.1053	0.0932

Table S2. Crystal data and structure refinement for compounds **4**-**5**.

	Compound **4**	Compound **5**
Empirical Formula	$C_{100}H_{92}Cd_4N_{12}O_{24}$	$C_{108}H_{92}Cd_4N_{12}O_{24}$
Formula Mass	2295.45	2391.53
Temperature/K	173.0	173.0
Wavelength/Å	1.54178	1.54178
Crystal system	Monoclinic	Monoclinic
Space group	*C*2/*c*	*C*2/*c*
θ/°	3.370 to 72.116	3.398 to 74.356°
a/Å	26.2410(8)	26.0598(6)
b/Å	7.6898(2)	8.2468(2)
c/Å	23.0522(7)	22.9568(6)
α/°	90	90
β/°	91.710(3)	93.4870(10)
γ/°	90	90
V/Å^3	4649.6(2)	4924.5(2)
Z	2	2
D_c/g·cm^{-3}	1.640	1.613
μ/ mm^{-1}	7.933	7.519
F(000)	2320	2416
R_1 (I >2σ(I))	0.0430	0.0275
wR_2 (all data)	0.1047	0.0734

Table S3. Selected bond lengths and angles in compound **1**.

Compound 1			
Cd(1)-O(1)	2.363(8)	O(6)#7-Cd(2)-O(16)#9	99.3(3)
Cd(1)-O(2)	2.452(8)	O(8)#8-Cd(2)-O(5)#7	80.4(3)
Cd(1)-O(3)#5	2.164(9)	O(8)#8-Cd(2)-O(7)#8	54.1(3)
Cd(1)-O(9)	2.353(8)	O(8)#8-Cd(2)-O(15)#9	88.2(3)
Cd(1)-O(10)	2.443(8)	O(14)-Cd(2)-O(5)#7	82.5(3)
Cd(1)-O(11)#6	2.319(8)	O(14)-Cd(2)-O(6)#7	113.9(3)
Cd(1)-O(12)#6	2.425(9)	O(14)-Cd(2)-O(7)#8	85.5(3)
Cd(2)-O(5)#7	2.467(8)	O(14)-Cd(2)-O(8)#8	138.1(3)
Cd(2)-O(6)#7	2.258(8)	O(14)-Cd(2)-O(15)#9	89.9(3)
Cd(2)-O(7)#8	2.518(8)	O(14)-Cd(2)-O(16)#9	97.3(3)
Cd(2)-O(8)#8	2.328(8)	O(15)#9-Cd(2)-O(5)#7	152.7(3)
Cd(2)-O(14)	2.248(9)	O(15)#9-Cd(2)-O(7)#8	72.5(3)
Cd(2)-O(15)#9	2.445(8)	O(16)#9-Cd(2)-O(5)#7	151.2(3)
Cd(2)-O(16)#9	2.319(8)	O(16)#9-Cd(2)-O(7)#8	128.0(3)
Cd(3)-O(2)#10	2.315(9)	O(16)#9-Cd(2)-O(8)#8	115.6(3)
Cd(3)-O(4)#11	2.238(8)	O(16)#9-Cd(2)-O(15)#9	55.7(3)
Cd(3)-O(7)#8	2.344(8)	O(2)#10-Cd(3)-O(7)#8	102.1(3)
Cd(3)-O(10)#10	2.331(7)	O(2)#10-Cd(3)-O(10)#10	77.5(3)
Cd(3)-O(13)	2.225(8)	O(4)#11-Cd(3)-O(2)#10	92.0(3)
Cd(3)-O(15)#9	2.305(9)	O(4)#11-Cd(3)-O(7)#8	85.3(3)
O(1)-Cd(1)-O(2)	53.4(3)	O(4)#11-Cd(3)-O(10)#10	94.3(3)
O(1)-Cd(1)-O(10)	125.4(3)	O(4)#11-Cd(3)-O(15)#9	160.3(3)
O(1)-Cd(1)-O(12)#6	146.3(3)	O(10)#10-Cd(3)-O(7)#8	179.4(3)
O(3)#5-Cd(1)-O(1)	94.3(4)	O(13)-Cd(3)-O(2)#10	160.7(3)
O(3)#5-Cd(1)-O(2)	89.0(3)	O(13)-Cd(3)-O(4)#11	100.8(3)

Symmetry transformations used to generate equivalent atoms: #5 x-1,y,z #6 x,y-1,z #7 x-1,y,z+1 #8 x-1,y+1,z+1 #9 x-1,y+1,z #10 -x,-y+2,-z+1 #11 -x+1,-y+2,-z+1

Table S4. Selected bond lengths and angles in compound **2**.

Compound 2			
Cd(1)-N(2)	2.319(3)	O(2)#4-Cd(1)-O(4)#5	95.23(11)
Cd(1)-O(1)	2.233(3)	O(2)#4-Cd(1)-N(2)	83.90(12)
Cd(1)-O(2)#4	2.251(3)	O(1)-Cd(1)-O(4)#5	135.42(12)
Cd(1)-O(3)#5	2.436(4)	N(2)-Cd(1)-N(3)#3	170.96(13)
O(2)#4-Cd(1)-N(3)#3	89.34(12)	N(2)-Cd(1)-O(3)#5	80.23(13)
O(1)-Cd(1)-O(2)#4	128.48(11)	N(2)-Cd(1)-O(4)#5	107.75(13)
O(2)#4-Cd(1)-O(3)#5	138.36(12)	N(3)#3-Cd(1)-O(3)#5	108.80(13)
O(1)-Cd(1)-O(3)#5	89.15(11)	O(4)#5-Cd(1)-N(3)#3	78.78(13)
O(1)-Cd(1)-N(3)#3	91.90(12)	O(4)#5-Cd(1)-O(3)#5	54.63(12)
O(1)-Cd(1)-N(2)	87.64(12)		
Symmetry transformations used to generate equivalent atoms: #3 x+1,y-1,z #4 -x+1,-y,-z+2 #5 x-1,y-1,z			

Table S5. Selected bond lengths and angles in compound **3**.

Compound 3			
Cd(1)-N(3)	2.277(3)	O(7)#4-Cd(1)-O(2)#2	93.03(10)
Cd(1)-O(1)	2.248(2)	O(7)#4-Cd(1)-O(3)#3	80.34(9)
Cd(1)-O(2)#2	2.283(2)	O(7)#4-Cd(1)-O(9)	90.30(10)
Cd(1)-O(3)#3	2.447(2)	O(9)-Cd(1)-N(3)	174.28(11)
Cd(1)-O(7)#4	2.253(3)	O(9)-Cd(1)-O(2)#2	86.32(9)
Cd(1)-O(9)	2.266(2)	O(9)-Cd(1)-O(3)#3	99.98(9)
N(3)-Cd(1)-O(2)#2	88.20(10)	O(1)-Cd(1)-O(7)#4	161.46(9)
N(3)-Cd(1)-O(3)#3	85.65(10)	O(1)-Cd(1)-O(9)	86.38(10)
O(1)-Cd(1)-N(3)	93.46(11)	O(2)#2-Cd(1)-O(3)#3	170.81(9)
O(1)-Cd(1)-O(2)#2	104.93(9)	O(7)#4-Cd(1)-N(3)	91.62(11)
O(1)-Cd(1)-O(3)#3	82.28(9)		
Symmetry transformations used to generate equivalent atoms: #2 -x+1,-y+1,-z #3 x,y+1,z #4 x,y+1,z-1			

Table S6. Selected bond lengths and angles in compound **4**.

Compound 4			
Cd(1)-O(5)	2.283(3)	O(1)-Cd(1)-O(4)#4	111.59(13)
Cd(1)-N(2)	2.253(4)	O(1)-Cd(1)-O(5)	99.11(14)
Cd(1)-O(1)	2.236(3)	O(4)#4-Cd(1)-O(2)	154.07(13)
Cd(1)-O(2)	2.465(4)	O(5)-Cd(1)-O(2)	119.15(14)
Cd(1)-O(3)#4	2.319(3)	O(5)-Cd(1)-O(3)#4	138.52(12)
Cd(1)-O(4)#4	2.397(3)	O(5)-Cd(1)-O(4)#4	83.33(12)
N(2)-Cd(1)-O(5)	89.49(13)	O(3)#4-Cd(1)-O(2)	100.49(14)
N(2)-Cd(1)-O(2)	88.13(12)	O(3)#4-Cd(1)-O(4)#4	55.39(11)
N(2)-Cd(1)-O(3)#4	104.35(13)	O(1)-Cd(1)-N(2)	142.19(13)
N(2)-Cd(1)-O(4)#4	105.93(13)	O(1)-Cd(1)-O(3)#4	93.30(14)
Symmetry transformations used to generate equivalent atoms: #4 -x+1/2,y-3/2,-z+1/2			

Table S7. Selected bond lengths and angles in compound **5**.

Compound 5			
Cd(1)-N(1)	2.2478(19)	O(1)-Cd(1)-O(3)#4	119.09(6)
Cd(1)-O(1)	2.2256(17)	O(1)-Cd(1)-O(4)#4	99.70(7)
Cd(1)-O(2)	2.4320(17)	O(1)-Cd(1)-O(5)	99.94(7)
Cd(1)-O(3)#4	2.4108(17)	O(5)-Cd(1)-O(4)#4	138.70(7)
Cd(1)-O(4)#4	2.3307(18)	N(1)-Cd(1)-O(5)	87.55(8)
Cd(1)-O(5)	2.2804(18)	O(4)#4-Cd(1)-O(3)#4	55.39(6)
N(1)-Cd(1)-O(4)#4	96.63(7)	O(5)-Cd(1)-O(2)	124.39(7)
O(1)-Cd(1)-N(1)	144.86(7)	O(3)#4-Cd(1)-O(2)	151.76(6)
O(1)-Cd(1)-O(2)	56.23(6)	O(5)-Cd(1)-O(3)#4	83.32(6)
N(1)-Cd(1)-O(2)	91.19(6)	N(1)-Cd(1)-O(3)#4	95.78(7)
O(4)#4-Cd(1)-O(2)	96.67(6)		
Symmetry transformations used to generate equivalent atoms: #4 -x+1/2,y-3/2,-z+1/2			

Reference

1. Sheldrick, G. M. A Short History of SHELX. Acta Crystallogr., Sect. A: Found. Crystallogr. 64, 112 (2008).